Spin- and charge-modulated trilayer magnetic junctions:

$La_{0.7}Ca_{0.3}MnO_3/La_{0.45}Ca_{0.55}MnO_3/La_{0.7}Ca_{0.3}MnO_3$

2003 J. Phys.: Condens. Matter 15 5243

(http://iopscience.iop.org/0953-8984/15/30/306)

INSTITUTE OF PHYSICS PUBLISHING JOURNAL OF PHYSICS: CONDENSED MATTER

J. Phys.: Condens. Matter **15** (2003) 5243–5251 PII: S0953-8984(03)62340-4

Spin- and charge-modulated trilayer magnetic junctions: $La_{0.7}Ca_{0.3}MnO_3/La_{0.45}Ca_{0.55}MnO_3/La_{0.7}Ca_{0.3}MnO_3$

Moon-Ho Jo[1], M G Blamire[1], D Ozkaya[2] and A K Petford-Long[2]

[1] Department of Materials Science, University of Cambridge, Pembroke Street, Cambridge CB2 3QZ, UK
[2] Department of Materials, University of Oxford, Parks Road, Oxford OX1 3PH, UK

E-mail: mhjo@fas.harvard.edu

Received 16 April 2003
Published 18 July 2003
Online at stacks.iop.org/JPhysCM/15/5243

Abstract

We report on magnetic tunnel junctions entirely made up of mixed-valence manganites, $La_{0.7}Ca_{0.3}MnO_3/La_{0.45}Ca_{0.55}MnO_3/La_{0.7}Ca_{0.3}MnO_3$. In heteroepitaxial junctions, the different Mn^{3+}/Mn^{4+} mixed-valence ratios can modulate the ground states throughout the trilayer, i.e. ferromagnetic metal/antiferromagnetic insulator/ferromagnetic metal. Interestingly, the tunnel magnetoresistance (TMR) of the device persists up to a higher temperature ($T/T_C \leqslant 0.75$, where T_C is the Curie temperature) as compared to the case for equivalent non-manganite barrier junctions. The enhanced TMR at high temperatures in the present junction is discussed in relation to the properties of the unique interface between the metallic ferromagnet and the antiferromagnetic tunnel barrier, such as the interfacial bonding coherence and a magnetic interlayer coupling.

Optimally doped manganites have been regarded as a good system in which to study spin-polarized tunnelling because of their half-metallic nature [1–5]. Indeed, magnetic tunnel junctions (MTJs) incorporating these materials have yielded reproducibly large tunnel magnetoresistances (TMRs) at low temperatures. Nevertheless, the TMR becomes suppressed drastically with increasing temperature and does not persist close to the Curie temperatures (T_C). A probable explanation can be found in the instability of the electronic and magnetic phase homogeneity of mixed-valence manganites [5]. Although the physical origin of phase separation in this class of materials is not fully understood yet, the tendency toward phase inhomogeneity appears to be more pronounced at surfaces and interfaces [6, 7]; this tendency is, in turn, critical for tunnelling. For example, local strain at interfaces [8] or a loss of cubic symmetry around the interfacial Mn ions [9] can suppress the bulk metallic ferromagnetism.

The mixed-valence manganites $La_{1-x}Ca_xMnO_3$ ($0 \leqslant x \leqslant 1$) exhibit diverse magnetic and electronic features over the entire range of doping as a result of the intricate interplay among their spin, charge, orbital and lattice degrees of freedom [10]. For the doping range $0.2 \leqslant x \leqslant 0.5$, the ground state of $La_{1-x}Ca_xMnO_3$ is a ferromagnetic (FM) metal, which can be qualitatively explained by the double-exchange interaction [11, 12]. In the higher-doping regimes with $x \geqslant 0.5$, the charges become localized by the ordering of Mn^{3+} and Mn^{4+} cations on specific lattice sites, which suppresses the double exchange and promotes an antiferromagnetic (AFM) insulating state.

An all-manganite trilayer LCMO/$La_{0.45}Ca_{0.55}MnO_3$ ($L_{0.45}C_{0.55}$MO)/LCMO junction is described here. The chosen barrier material $L_{0.45}C_{0.55}$MO is known to be an AFM insulator in the ground state (Néel temperature: ∼210 K for a bulk crystal) passing via a charge-ordered insulator phase from a paramagnetic insulator at higher temperatures. In the heteroepitaxial junction the different Mn^{3+}/Mn^{4+} mixed-valence ratios can modulate the *electrical* and *magnetic* properties throughout the trilayer, i.e. FM metal/AFM insulator/FM metal, while the bulk crystal symmetry of Mn ions in the LCMO will be coherently preserved at interfaces; i.e. the perovskite lattice structure is preserved throughout the heterostructure: the in-plane lattice mismatch is as small as <0.3%.

LCMO/$L_{0.45}C_{0.55}$MO/LCMO trilayers were grown *in situ* on (001) $NdGaO_3$ (NGO) by pulsed laser deposition (KrF laser, 248 nm) using stoichiometric targets with the layer thicknesses of 60 nm/3–7 nm/80 nm [5, 8]. In figure 1, a high-resolution cross-sectional transmission electron microscope image obtained near the interface demonstrates the good heteroepitaxial quality of the trilayer. The energy-filtered line profile (averaged over 400 lines in the box) of the Ca $L_{2,3}$ energy loss edge across the barrier reveals the appropriate chemical modulation of the Ca ions at the interface [13]. The overall chemical compositions and magnetic structures for each layer were also confirmed for separate thin films. A surface atomic force microscope scan shown in the inset also shows a typical layer-by-layer growth mode, further confirming that the interfaces are atomically flat. Devices were patterned using optical lithography and Ar ion milling to produce micron-scale square mesas. Electrical measurements of the junctions were performed using four-terminal ac measurements and magnetic measurements were made with a commercial SQUID magnetometer. For all the measurements in this study, the magnetic field was applied parallel to the plane of the samples.

Figure 2 shows the magnetic field-dependent TMR measured at various temperatures above 77 K. It displays distinct binary resistance states with sharp switching, where the maximum TMR defined as $(R_{ap} - R_p)/R_{ap}$ is 16.7% at 77 K and is suppressed to about 1% at 200 K, where R_{ap} and R_p represent the junction resistances when the two ferromagnets have antiparallel and parallel magnetizations—note that the TMR here is defined as $(R_{ap} - R_p)/R_{ap}$. We note that the temperature-dependent junction resistance is not dominated by the highly insulating barrier, as we often observed in other manganite junctions with non-manganite tunnel barriers such as $SrTiO_3$ (STO) [1] or $NdGaO_3$ (NGO) [5], where the junction resistances show thermally activated behaviours. However, the junction specific resistance (the product of the resistance and the junction area) was approximately constant for junction sizes from 6×6 to 20×30 μm^2 and also systematically scales with the barrier thickness from 3 to 7 nm. The dynamic conductance (dV/dI) of the junction versus the applied bias voltage shows a quadratic dependence at all measurement temperatures as shown in the inset of figure 2 and thus it is not inconsistent with the view that the majority of the conduction of the junction arises by a tunnelling process.

$La_{1-x}Ca_xMnO_3$ at $x \sim 0.5$, which lies at the phase boundary between the FM metallic state ($x < 0.5$) and the charge-ordered AFM insulating state ($x > 0.5$) has attracted considerable interest, mainly because of the strong competition between two dissimilar phases. Indeed the

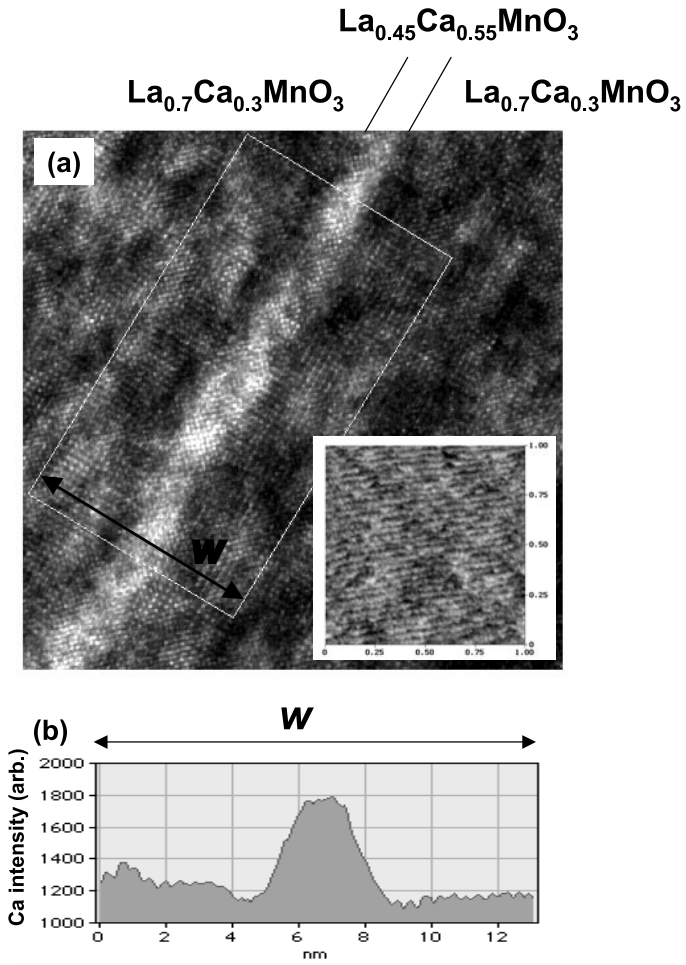

Figure 1. (a) The cross-sectional high-resolution transmission electron microscope (TEM) image of the LCMO/$L_{0.45}C_{0.55}$MnO/LCMO trilayer and (b) an energy filter TEM line profile (400) of the Ca $L_{2,3}$ energy loss edge across the barrier (averaged over 400 lines in the box). In the inset of (a) the AFM surface image of the trilayer shows the layer-by-layer growth, maintaining a typical step and terrace feature of a pseudocubic perovskite.

physical properties of $La_{1-x}Ca_xMnO_3$ near $x \sim 0.5$ are very sensitive to the slight variation of x [14, 15]. Experimental evidence relating to these compositions strongly suggested the coexistence of FM metallic and charge-ordered AFM insulating phases on the microscopic length scale (∼nm) even at low temperatures[3]. In this study we have verified that a 60 nm thick $L_{0.45}C_{0.55}$MO layer shows a *macroscopically* insulating behaviour at low temperatures, by measuring in-plane current between electrical contacts 8 mm apart. Nevertheless, the *mesoscopic* conductance across the finite length of such an inhomogeneous system can be qualitatively different. In particular, when the conduction length is comparable to the size of the segregated phases on the nanometre scale, i.e. in the 3–7 nm thick barriers of the present junctions, it is likely that the junction conductance will be subject to phase fluctuations within

[3] For example, see the references in [6] and [7].

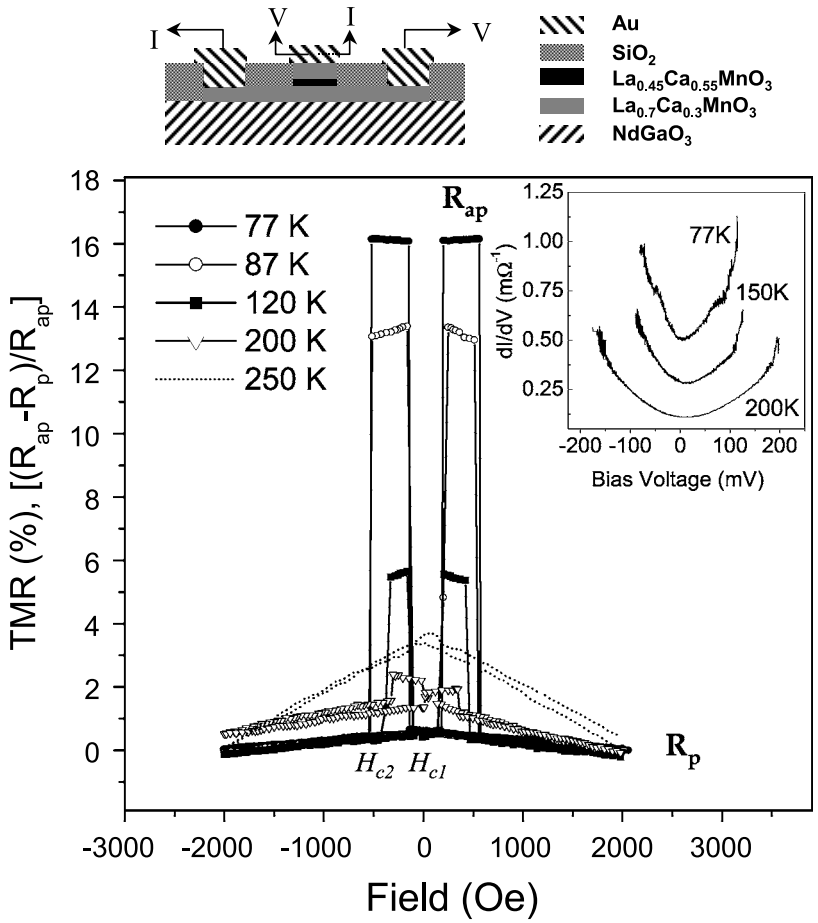

Figure 2. The TMR defined as $(R_j - R_{ap})/R_{ap}$ (%) at different temperatures. The measurable TMR persists up to 200 K and at 250 K it only shows the background from the electrode. The inset shows the dynamic conductance of the junction, $\mathrm{d}I/\mathrm{d}V$, versus the bias voltage at zero field at different temperatures. All curves can be fitted by quadratic functions, $\mathrm{d}I/\mathrm{d}V = A + BV^2$, where A and B are constants which depend on the temperature.

the barrier. Consequently the junction conductance will noticeably deviate from an elastic tunnelling process, giving rise to the suppressed TMR as in the present junction.

In figure 3 the temperature dependence of the TMR of the present junction is compared to those of other manganite-based junctions with non-magnetic barriers from the literature—see [1] and [5]. The maximum TMR at low temperatures in the junction is lower than those in other junctions—the TMR is 86% for LCMO/NGO/LCMO at 77 K [5] and 45% for $La_{0.67}Sr_{0.33}MnO_3$/STO/$La_{0.67}Sr_{0.33}MnO_3$ at 4.2 K [1]. Nevertheless it is very interesting to note that the TMR decreases less steeply and persists up to higher temperatures: above 120 K the TMR of the present junction is actually *higher* than those of other junctions—see also the normalized TMR in the inset for clarity—and it also retains a distinct MR effect with a binary switching up to 200 K (figure 2). *It is this temperature dependence of the TMR that we concentrate on in the following*. In order to investigate interfacial magnetism in LCMO/$L_{0.45}C_{0.55}$MO/LCMO trilayers we performed further magnetic measurements.

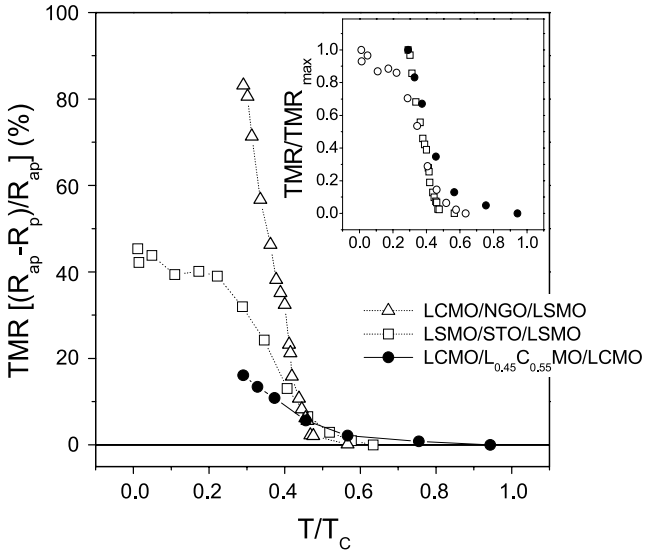

Figure 3. The TMR versus temperature for the present junction (a manganite barrier) and those of junctions with non-manganite barriers. LSMO/STO/LSMO and LCMO/NGO/LCMO stand for $La_{0.67}Sr_{0.33}MnO_3/SrTiO_3/La_{0.67}Sr_{0.33}MnO_3$ and $La_{0.7}Ca_{0.3}MnO_3/NdGaO_3/La_{0.7}Ca_{0.3}MnO_3$, as studied in [1] and [5], respectively. The inset shows the normalized TMR/TMR$_{max}$ versus temperature for clarity.

It should be noted that here we mainly chose *unpatterned* (5×10 mm^2) heteroepitaxial trilayers grown on STO(001) rather than ones grown on NGO(001), because these can avoid strong background paramagnetism from Nd^{3+} ($J = 9/2$) during the magnetic measurements.

The temperature dependence of the TMR in the manganite junctions depends strongly on the nature of the FM metal/insulator interface. The devices described here differ from those with non-manganite barriers in two key aspects. Firstly, the structural and chemical coherence of the interface may preserve the interfacial FM order of the LCMO electrodes: the quasi-continuous interfacial Mn–O–Mn bonds are preserved across the interface without a significant modification of the symmetry of the Mn ions. Secondly, the interfacial magnetism in the LCMO/$L_{0.45}C_{0.55}$MO/LCMO junction, in which the barrier is magnetic, is also different from those in the junctions with non-manganite barriers. In our study, the magnetic properties of $L_{0.45}C_{0.55}$MO, characterized by a plain 60 nm thick film, suggest that it is a canted antiferromagnet at low temperatures: it shows an ordering peak at $\sim$200 K in the temperature-dependent magnetization; also, the magnetization–field curves exhibit a small hysteresis with a saturation magnetic moment at 10 K that is 1.6% of that for the same thickness of LCMO. Since the barrier is AFM, there is the possibility of an interlayer coupling between LCMO and $L_{0.45}C_{0.55}$MO—for example, a self-biased exchange interaction between FM electrodes and an AFM insulator below their ordering temperatures [16]. Exchange bias in FM/AFM bilayer systems has attracted wide interest as regards applications in magnetic recording heads [17] and MTJs [18] because it can provide a unidirectional anisotropy and stabilize the FM domain structure. Phenomenologically, the asymmetrical magnetization (M)–field (H) hysteresis is generally accompanied by an enhanced coercivity in the FM due to an interfacial interaction with the AFM part [19]. We did indeed observe asymmetrical M–H hysteresis loops when the sample was cooled in the presence of an external magnetic field, as shown in figure 4. We first note that the magnetization reversal is asymmetric when H_{FC} is zero or relatively small—see

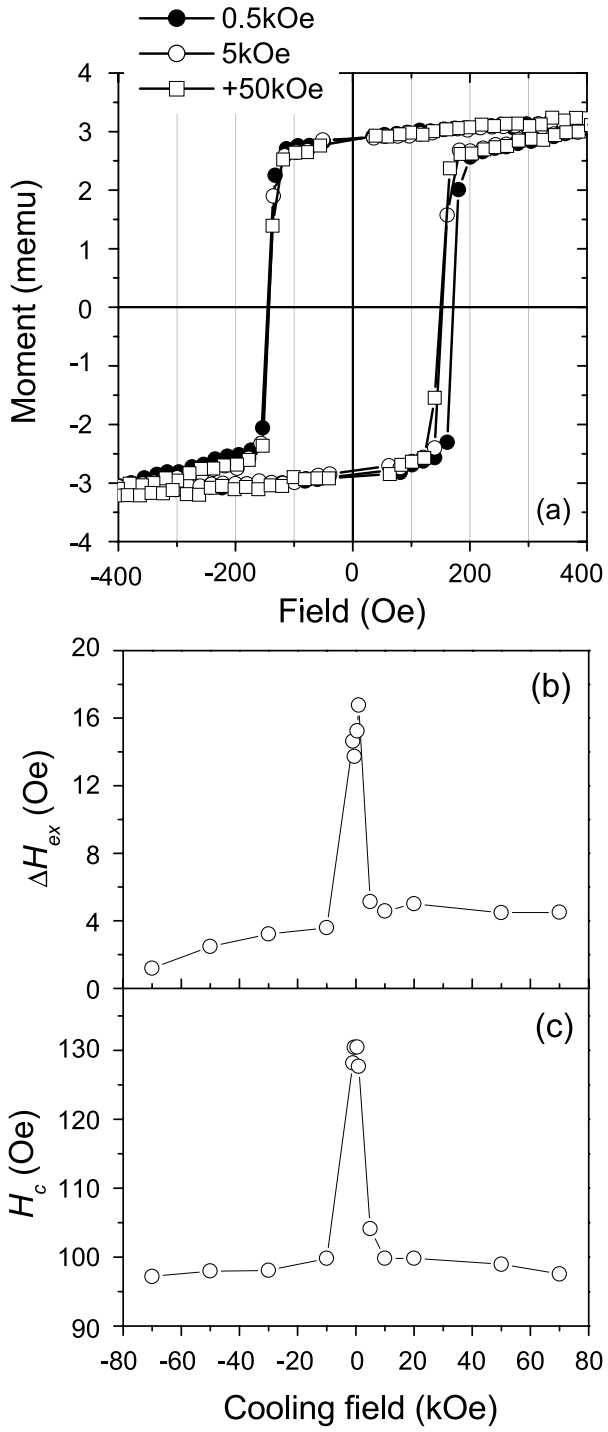

Figure 4. (a) A typical M–H loop for the unpatterned LCMO/$L_{0.45}C_{0.55}$MnO/LCMO trilayer in different cooling fields (H_{FC}) at 77 K. (b) The shift in the M–H loops ($\Delta H_{ex} \equiv (H_c^+ + H_c^-)/2$) and (c) the coercivity ($\Delta H_c \equiv (H_c^+ - H_c^-)/2$) at 77 K as a function of H_{FC}. Here H_c^+ is H_c when the field is reversed from positive to negative and H_c^- is H_c when the field is reversed from negative to positive.

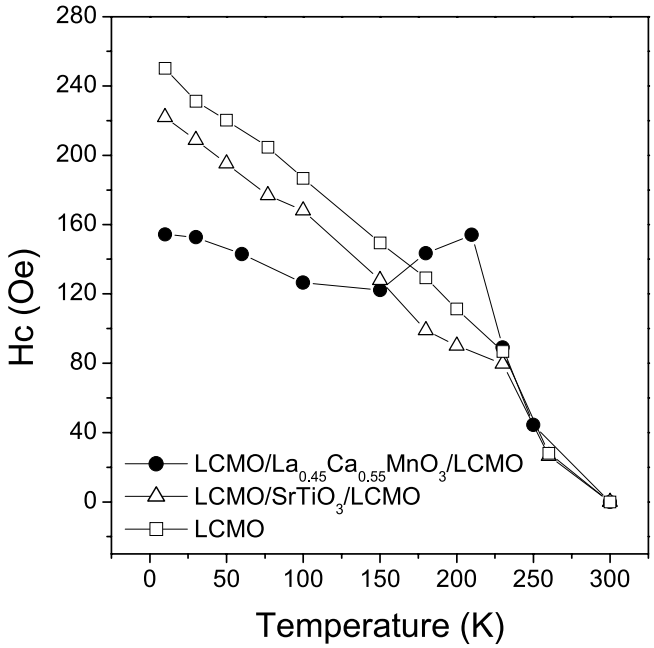

Figure 5. The temperature-dependent field H_c in an unpatterned LCMO/$L_{0.45}C_{0.55}$MnO/LCMO trilayer, an unpatterned LCMO/$SrTiO_3$/LCMO trilayer and a plain LCMO film.

the case where H_{FC} (the applied field during cooling) is 0.5 kOe in figure 4(a): it shows dissimilar coercivities (H_c) when the field is reversed from positive to negative (H_c^+) and from negative to positive (H_c^-). This asymmetry was reproducibly observed and persists until the hysteresis disappears at high temperatures. It was revealed that the asymmetry ($\Delta H_{ex} \equiv (H_c^+ + H_c^-)/2$) is strongly dependent on H_{FC}, as shown in figure 4(b); however, it should be noted that the sign of ΔH_{ex} is not dependent on the polarity of the external cooling field but instead on the sample orientation with respect to the external field. It is qualitatively different from the normal exchange bias, where the sign of ΔH_{ex} follows the polarity of the external cooling field. The H_{FC}-dependence of the coercivity H_c, defined as $H_c \equiv (H_c^+ - H_c^-)/2$, is shown in figure 4(c) and it exhibits an essentially similar variation to H_{ex}, suggesting a common physical basis. Similar measurements have been made on a plain LCMO film and H_c is only weakly dependent on H_{FC}, as expected for a conventional ferromagnet. Therefore it is clear that the observed H_{FC}-dependence of ΔH_{ex} and H_c in the trilayers is due to the presence of the AFM $L_{0.45}C_{0.55}$MO barrier.

The temperature-dependent field H_c measured for the LCMO/$L_{0.45}C_{0.55}$MO/LCMO (unpatterned) film is shown along with those for an LCMO/$SrTiO_3$/LCMO (unpatterned) film and a plain LCMO film in figure 5 and it distinctly exhibits a strong enhancement of H_c at $\sim$200 K, which is close to T_N for $L_{0.45}C_{0.55}$MO. This further corroborates the assertion that the magnetic reversal of the LCMO/$L_{0.45}C_{0.55}$MO/LCMO trilayer is strongly influenced by the presence of the AFM $L_{0.45}C_{0.55}$MO barrier.

A similar coercivity enhancement is often observed in exchange bias bilayers and is attributed to both instabilities of the AFM layers and inhomogeneous reversal of the FM [20]. The aforementioned observed magnetic features such as asymmetric magnetization reversal and the H_c-enhancement near T_N in our study can be further considered, particularly as

regards the role of the AFM $L_{0.45}C_{0.55}MO$ barrier, as follows. In conventional *macroscopic* exchange bias systems [21], it is assumed that the AFM anisotropy is sufficiently large compared to the FM anisotropy and the interfacial exchange coupling constant (J_{INT}), i.e. $K_{AFM}t_{AFM} \gg K_{FM}t_{FM}$ and $K_{AFM}t_{AFM} \gg J_{INT}$, where K_i and t_i are the anisotropy constant and the thickness of the respective layers. However, if either J_{INT} and/or $K_{FM}t_{FM}$ is comparable to $K_{AFM}t_{AFM}$, i.e. $t_{FM} \gg t_{AFM}$, the magnetization reversal cannot be effectively exchange biased on the *macroscopic* level. Instead, the FM and AFM spins can be coupled; for example, they can be reversed together. Then overall magnetization reversal can be influenced by the magnetic AFM microstructures, i.e. the AFM domain structures [22] or crystal orientation [23]. In fact, a direct observation of the *microscopic* features of an exchange bias system $Co/LaFeO_3$ reveals that the FM–AFM exchange bias can be a local domain-by-domain interaction; the FM spin directions are locally determined by the spin directions in the underlying AFM layers [24]. An asymmetric magnetization reversal was observed in Fe/MnO_2 bilayers and it was ascribed to the coupling between the magnetization of Fe and the twinned crystal structure of the AFM (110) MnO_2 [25]. It should be noted that in our study the sign of ΔH_{ex} was only dependent on the sample orientation with respect to H_{FC}, not on the polarity of H_{FC}. This suggests that the similar origin related to the twinned crystal structure of the barrier with an orthorhombic symmetry, which is commonly observed in $La_{1-x}Ca_xMnO_3$ with $x \sim 0.5$ [26], causes a similar asymmetric reversal in this study.

The magnetic structure of $L_{0.45}C_{0.55}MO$ tends to be a multi-phase mixture, i.e. nanometre-size FM clusters in the AFM matrix at the ground state as discussed above, and this tendency towards phase separation is more pronounced near the magnetic transition temperature [27], i.e. T_N. A similar coercivity enhancement was reported in an MnF_2/Fe exchange bias bilayer and it was attributed as being due to the interfacial frustration in AFM MnF_2 driven by H_{FC}, which effectively pins the propagating domain wall motions in the Fe [24]. The H_c-enhancement of LCMO near T_N for $L_{0.45}C_{0.55}MO$ can be understood as the stabilization of the domain structure of the LCMO due to the local pinning torque originating from the maximum magnetic inhomogeneity or frustration in AFM $L_{0.45}C_{0.55}MO$ at its magnetic transition.

We argue that the H_c-enhancement of LCMO near T_N for the $L_{0.45}C_{0.55}MO$ in our study is evidence of a strong exchange coupling between the AFM barrier and the FM electrodes which persists up to their ordering temperatures. This demonstrates that the LCMO interface remains FM above 200 K. This exchange interaction with the barrier therefore provides a plausible explanation for the improved high-temperature performance of this device structure.

MTJs based on transition metal oxides such as Fe_3O_4 and CrO_2 can be built utilizing their high spin polarization; we note that these materials are closely related to AFM insulators of different oxygen coordination such as Fe_2O_3 and Cr_3O_4. The present work could have implications for the further development of such MTJs, where the role of magnetically active barriers can be exploited.

Acknowledgments

This work was supported by the EPSRC through the Advanced Magnetics Programme and the UK–Korea Science & Technology Collaboration Fund.

References

[1] Lu Y, Li X W, Gong G Q, Xiao G, Gupta A, Lecoeur P, Sun J Z, Wang Y Y and Dravid V P 1996 *Phys. Rev.* B **54** 8357

Sun J Z, Gallagher W J, Duncombe P R, Krusin-Elbaum L, Altman R A, Gupta A, Lu Y, Gong G Q and Xiao G 1996 *Appl. Phys. Lett.* **69** 3266

[2] Viret M, Drouet M, Nassar J, Coutour J P, Fermon C and Fert A 1997 *Europhys. Lett.* **39** 545
[3] Obata T, Manako T, Shimakawa Y and Kubo Y 1999 *Appl. Phys. Lett.* **74** 290
[4] O'Donnell J, Andrus A E, Oh S, Collar V and Eckstein J N 1999 *Appl. Phys. Lett.* **76** 1914
[5] Jo M-H, Mathur N D, Todd N K and Blamire M G 2000 *Phys. Rev.* B **61** R14905
[6] Moreo A, Yunoki S and Dagotto E 1999 *Science* **283** 2034
Dagotto E, Hotta T and Moreo A 2000 *Preprint* cond-mat/0012117
[7] Mathur N D and Littlewood P B 2001 *Solid State Commun.* **119** 271
[8] Jo M-H, Mathur N D, Eveтts J E and Blamire M G 1999 *Appl. Phys. Lett.* **75** 3689
[9] Calderón M J, Brey L and Guinea F 1999 *Phys. Rev.* B **60** 6698
[10] For a review, see
Salamon M B and Jaime M 2001 *Rev. Mod. Phys.* **73** 583
Coey J M D, Viret M and von Molnár S 1999 *Adv. Phys.* **48** 167
[11] Zener C 1951 *Phys. Rev.* **82** 403
[12] Anderson P W and Hasegawa H 1955 *Phys. Rev.* **100** 675
[13] Ozkaya D, Petford-Long A K, Jo M-H and Blamire M G 2001 *J. Appl. Phys.* **89** 6757
[14] Roy M, Mitchell J F, Ramirez A P and Schiffer P 1999 *J. Phys.: Condens. Matter* **11** 4834
[15] Huang Q, Lynn J W, Erwin R W, Santoro A, Dender D C, Smolyaninova V N, Ghosh K and Greens R L 2000 *Phys. Rev.* B **61** 8895
[16] Krivorotov I N *et al* 2001 *J. Appl. Phys.* **89** 6964
Panagiotopoulos I *et al* 1999 *Phys. Rev.* B **60** 485
[17] Dieny B, Speriosu V S, Parkin S S P, Gurney B A, Wilhoit D R and Mauri D 1991 *Phys. Rev.* B **43** 1297
[18] Gallagher W J, Parkin S S P, Lu Y, Bian X P, Marley A C, Roche K P, Altman R A, Rishton S, Jahnes C, Shaw T M and Xiao G 1997 *J. Appl. Phys.* **81** 3741
[19] Stiles M D and McMichael R D 2001 *Phys. Rev.* B **63** 064405
[20] Leighton C, Nogues J, Jönsson-Åkerman B J and Schuller I K 2000 *Phys. Rev. Lett.* **84** 3466
[21] Nogues J and Schuller I K 1999 *J. Magn. Magn. Mater.* **192** 203
[22] Zhou S M, Liu K and Chien C L 1998 *Phys. Rev.* B **58** 14717
[23] Nogues J, Morgan T J, Lederman D, Schuller I K and Rao K V 1999 *Phys. Rev.* B **59** 6984
[24] Nolting F, Scholl A, Stöhr J, Seo J W, Fompeyrine J, Siegwart H, Locquet J-P, Anders S, Lünling J, Fullerton E E, Toney M F, Scheinfein M R and Padmore H A 2000 *Nature* **405** 767
[25] Fitzsimmons M R, Yashar P, Leighton C, Schuller I K, Nogues J, Majkrzak C F and Dura J A 2000 *Phys. Rev. Lett.* **84** 3986
Leighton C, Song M, Nogues J, Cyrille M C and Schuller I K 2000 *J. Appl. Phys.* **88** 344
[26] For direct visual evidence, see
Mori S, Chen C H and Cheong S-W 1998 *Nature* **392** 473
Chen C H and Cheong S-W 1996 *Phys. Rev. Lett.* **76** 4042
[27] Allodi G, De Renzi R, Licci F and Pieper M W 1998 *Phys. Rev. Lett.* **81** 4736